7-6-2010

Avirulent Uracil Auxotrophs Based on Disruption of Orotidine-5′-Monophosphate Decarboxylase Elicit Protective Immunity to Toxoplasma gondii

Barbara A. Fox
Dartmouth College

David J. Bzik
Dartmouth College

INFECTION AND IMMUNITY, Sept. 2010, p. 3744–3752 Vol. 78, No. 9
0019-9567/10/$12.00 doi:10.1128/IAI.00287-10

Avirulent Uracil Auxotrophs Based on Disruption of Orotidine-5′-Monophosphate Decarboxylase Elicit Protective Immunity to *Toxoplasma gondii*▽†

Barbara A. Fox* and David J. Bzik*

Department of Microbiology and Immunology, Dartmouth Medical School, 1 Medical Center Drive, Lebanon, New Hampshire 03756

Received 22 March 2010/Returned for modification 25 April 2010/Accepted 27 June 2010

The orotidine-5′-monophosphate decarboxylase (OMPDC) gene, encoding the final enzyme of the *de novo* pyrimidine biosynthesis pathway, was deleted using *Toxoplasma gondii* KU80 knockouts to develop an avirulent nonreverting pyrimidine auxotroph strain. Additionally, to functionally address the role of the pyrimidine salvage pathway, the uridine phosphorylase (UP) salvage activity was knocked out and a double knockout of UP and OMPDC was also constructed. The nonreverting ΔOMPDC, ΔUP, and ΔOMPDC ΔUP knockout strains were evaluated for pyrimidine auxotrophy, for attenuation of virulence, and for their ability to elicit potent immunity to reinfection. The ΔUP knockout strain was replication competent and virulent. In contrast, the ΔOMPDC and ΔOMPDC ΔUP strains were uracil auxotrophs that rapidly lost their viability during pyrimidine starvation. Replication of the ΔOMPDC strain but not the ΔOMPDC ΔUP strain was also partially rescued *in vitro* with uridine or cytidine supplementation. Compared to their hypervirulent parental type I strain, the ΔOMPDC and ΔOMPDC ΔUP knockout strains exhibited extreme attenuation in murine virulence (~8 logs). Genetic complementation of the ΔOMPDC strain using a functional OMPDC allele restored normal replication and type I parental strain virulence phenotypes. A single immunization of mice with either the live critically attenuated ΔOMPDC strain or the ΔOMPDC ΔUP knockout strain effectively induced potent protective immunity to lethal challenge infection. The avirulent nonreverting ΔOMPDC and ΔOMPDC ΔUP strains provide new tools for the dissection of the host response to infection and are promising candidates for safe and effective Th1 vaccine platforms that can be easily genetically engineered.

Toxoplasma gondii is an obligate intracellular protozoan parasite that invades and replicates in a wide variety of cell types. Infections are widespread in humans, and while infections in healthy individuals are typically asymptomatic, severe disease can occur *in utero* or in individuals with severe immune suppression (22, 29, 31). A chronic infection is established and is characterized by quiescent cysts containing bradyzoites in tissues such as brain, muscle, and eye (42). Chronic infection can reactivate in AIDS and cause toxoplasmic encephalitis (9, 31) or recurrent ocular toxoplasmosis, recently recognized as a prevalent retinal infection in the United States (23, 27). Current treatments are poorly tolerated and are ineffective against chronic stages of infection, and there are no vaccines. Targeting of the *T. gondii de novo* pyrimidine synthesis pathway is one potential approach to developing more-effective vaccination strategies based on live attenuated strains with defined genetic disruptions (14).

The key uracil phosphoribosyltransferase (UPRT) activity in the pyrimidine salvage pathway can easily be disrupted, and loss of UPRT has no apparent effect on parasite growth *in vitro* or virulence *in vivo* (4, 8). In the absence of any pyrimidine salvage pathway, *T. gondii* still possesses a complete six-step pathway for the *de novo* biosynthesis of UMP, the precursor molecule of all essential pyrimidines (1, 14, 34, 38). Insertional disruption of the first step of the biosynthetic pathway, encoded by the carbamoyl phosphate synthetase II (CPSII) gene, produced a severe uracil auxotrophy exemplified by the cps1-1 strain of *T. gondii*, which was incapable of *de novo* pyrimidine synthesis (13, 16). After invasion of a host cell, the cps1-1 uracil auxotrophic mutant was starved for pyrimidines and ceased to proliferate, since uracil is not readily available for salvage in mammals (12, 13, 32). The cps1-1 mutant strain also exhibited an extreme attenuation of virulence in both immune-competent and severely immune-deficient homozygous gamma interferon (IFN-γ) knockout mice (13).

Immunization of mice with the live attenuated type I cps1-1 strain elicits a potent $CD8^+$ T-cell-dependent lifelong protective immunity against infection with type I strains (13, 18) and against infection with type II strains and chronic infection (19). In contrast, immunization with *T. gondii* extracts or killed noninvasive intact parasites does not elicit significant immunity to reinfection with *T. gondii* (2, 40). Only actively infected host cells have been shown to prime $CD8^+$ T-cell-dependent immunity in *T. gondii* infection (10, 20, 21).

Immunity is effectively elicited by immunization with the cps1-1 strain in C57BL/6 (18), BALB/c (13), and $tyk2^{-/-}$ signaling-deficient mice (39) and surprisingly also in $MyD88^{-/-}$ deficient mice (41). Remarkably, macrophages primed *in vivo* by cps1-1 immunization but not naive macrophages also exhibit extremely efficient *ex vivo* IFN-γ-mediated innate cellular immunity augmenting intracellular rupture and clearance of type II and type III strains of *T. gondii* (30, 45–47), whereas virulent

* Corresponding author. Mailing address: Department of Microbiology and Immunology, Dartmouth Medical School, 1 Medical Center Drive, Lebanon, NH 03756. Phone: (603) 650-7951. Fax: (603) 650-6223. E-mail for David J. Bzik: david.j.bzik@dartmouth.edu. E-mail for Barbara A. Fox: barbara.a.fox@dartmouth.edu.

† Supplemental material for this article may be found at http://iai.asm.org/.

▽ Published ahead of print on 6 July 2010.

TABLE 1. Strains used in this study

Strain	Parent	Source or reference
RH	RH(ERP)	36, 37
RHΔ*ku80*::*HXGPRT*	RHΔ*hxgprt*	17
RHΔ*ku80*Δ*hxgprt*	RHΔ*ku80*::*HXGPRT*	17
RHΔ*ku80*Δ*ompdc*::*HXGPRT*	RHΔ*ku80*Δ*hxgprt*	This study
RHΔ*ku80*Δ*up*::*HXGPRT*	RHΔ*ku80*Δ*hxgprt*	This study
RHΔ*ku80*Δ*ompdc*Δ*hxgprt*	RHΔ*ku80*Δ*ompdc*::*HXGPRT*	This study
RHΔ*ku80*Δ*ompdc*Δ*up*::*HXGPRT*	RHΔ*ku80*Δ*ompdc*Δ*hxgprt*	This study
RHΔ*ku80*Δ*ompdc*::*HXGPRT*Δ*uprt*::*gOMPDC*	RHΔ*ku80*Δ*ompdc*::*HXGPRT*	This study

type I strains resist this cps1-1-induced innate killing mechanism (46).

The lifelong immunity elicited by vaccination with strain cps1-1 is dependent on $CD8^+$ T cells and interleukin 12 (IL-12) (41, 44) and is also dependent on IFN-γ (13, 18), although systemic IFN-γ is not required for priming (18). Surprisingly, cps1-1 rapidly elicits functional IL-12p70 both locally and systemically following vaccination (18). In contrast to current models of viral or intracellular bacterial infections, $CD8^+$ T-cell-intrinsic IL-12 signaling is required for development of IFN-γ-producing $CD8^+$ cytotoxic-T-lymphocyte populations and for the generation of memory $CD8^+$ T cells in response to cps1-1 (43, 44). Vaccination with cps1-1 induced four distinct effector $CD8^+$ T-cell types based on KLRG1 and CD62L expression levels (44). The rapidly elicited and abundant populations of antigen-specific effector $CD8^+$ T cells induced by vaccination with cps1-1 are cytolytic *in vitro* and *in vivo* (28). The nonreplicating cps1-1 vaccine model has significantly advanced the understanding of the host response, innate immunity, and protective adaptive immunity to *T. gondii* infection (3, 10, 13, 18, 19, 28, 30, 39, 41, 43–47).

The cps1-1 strain is not easily amenable to further genetic manipulation, and this strain exhibits an extremely low frequency of reversion to the virulent parental (strain RH) phenotype (13). To further address the potential of the six-step pyrimidine synthesis pathway to develop improved avirulent, nonreverting, genetically defined, and genetically manipulatable strains, we deleted the sixth and final enzyme of the pathway by targeted disruption of the orotidine-5′-monophosphate (OMP) decarboxylase, the OMPDC gene, in the RH strain KU80 knockout background, which now enables highly efficient gene targeting (17, 24). Targeted disruption of OMPDC via double-crossover homologous recombination induced severe pyrimidine auxotrophy and resulted in the generation of nonreverting strains that were essentially completely attenuated in their virulence in mice. A single immunization with ΔOMPDC knockout strains effectively induced a potent protective immunity to subsequent lethal challenge infection with *T. gondii*.

MATERIALS AND METHODS

Primers. All oligonucleotide primers used in this study for targeting plasmid construction and PCR validation of knockout genotypes are given in Table S1 and Table S2 in the supplemental material.

Plasmid constructs. All plasmids were based on the yeast shuttle vector pRS416, which was employed in a yeast recombinational cloning system (33). Briefly, recombination to fuse 3 distinct genetic elements (a 5′ target flank, a hypoxanthine-xanthine-guanine phosphoribosyltransferase [HXGPRT] selectable marker, and a 3′ target flank) in their correct order with pRS416 was performed using 31- to 34-bp crossovers common to pRS416, to the HXGPRT minicassette, or to gene targeting flanks (see Table S1 in the supplemental material) as required for yeast recombinational cloning (33). The knockout targeting plasmids were engineered to delete a small amount of the gene's predicted 5′ untranslated region (UTR) and essentially the entire predicted coding region of the targeted genomic locus. Targeting plasmids were verified by restriction enzyme digest and were then sequenced to verify 100% gene homology in targeting DNA flanks.

Plasmid pOMT2-2 was constructed to delete nucleotides 2715149 to 2718446 in the OMPDC locus, defined as TGGT1_010340 (55.m04842) on chromosome VIIb (chrVIIb) of the toxodb database (www.toxodb.org) (version 5.0). The HXGPRT minigene cassette (6, 7) was fused between a 1,055-bp 5′ genomic targeting flank and a 994-bp 3′ genomic targeting flank amplified from DNA isolated from the RHΔ*ku80*::*HXGPRT* strain (17).

Plasmid pOMC2-4 was constructed to remove HXGPRT from the chromosomal locus of strain RHΔ*ku80*Δ*ompdc*::*hxgprt* (Table 1). Plasmid pOMT2-2 was digested with PmeI to release the HXGPRT cassette fragment, followed by self-religation.

Plasmid pNUPT1-1 was designed to delete nucleotides 1108479 to 1111669 of the uridine phosphorylase (UP) locus on chrXI, annotated as TGGT1_086870. The HXGPRT minigene cassette was fused between a 1,024-bp 5′ targeting fragment and a 934-bp3′ targeting fragment.

Plasmid pGUPROMT was designed to complement uracil auxotrophy and disrupt UPRT. A chromosomal segment of 3,229 bp corresponding to nucleotides 2714788 to 2718017 on chrVIIb (the OMPDC gene) was flanked with a 1,131-bp 5′ UPRT-targeting DNA flank and a 1,119-bp 3′ UPRT-targeting DNA flank. Plasmid pGUPROMT was designed to replace nucleotides 2329098 to 2333188 of the annotated UPRT chromosomal locus, TGGT1_088770.

Strains, culture conditions, and plaque assays. The parental strains of *T. gondii* used in this study are RH (37) and the KU80 knockout strains RHΔ*ku80*::*hxgprt* and RHΔ*ku80*Δ*hxgprt* (17). All strains used in this study are listed in Table 1. Parasites were maintained by serial passage in diploid human foreskin fibroblasts (HFF) at 35°C (13). PFU assays were performed over 7 days (36) unless otherwise stated. Uracil, uridine, cytidine, deoxyuridine, deoxycytidine, xanthine, mycophenolic acid (MPA), and 5-fluorodeoxyuridine (FUDR) were obtained from Sigma Inc., while 6-thioxanthine (6TX) was obtained from Acros Organics (Thermo Fisher Scientific).

Pyrimidine starvation viability assays. Pyrimidine auxotrophs were inoculated into two groups of 25-cm^2 HFF flasks, where one set of flasks was seeded with ~100 to 200 PFU (low dose) and the second set was seeded with ~1,000 to 2,000 PFU (high dose). Parasites were allowed to invade for 2 h in uracil medium and were then rinsed three times with cold phosphate-buffered saline (PBS) to remove uracil and extracellular parasites. Groups of three flasks from the low-dose and high-dose groups were then provided with uracil medium to establish the initial viability (day 0) measured by PFU assay without pyrimidine starvation. The remaining flasks were then incubated in medium lacking uracil to induce pyrimidine starvation. At different times (1, 3, or 5 days) after initiation of pyrimidine starvation, parasites in 3 flasks from the low-dose group and in 3 flasks from the high-dose group were rinsed with cold PBS and then provided with uracil medium to establish viability as measured by PFU assay. The percentage of initial viability remaining after different times of pyrimidine starvation was determined from PFU counts. PFU data were subjected to a Student *t* test and are represented as the means ± the standard errors of the means (SEM).

Genomic DNA isolation and PCR. Genomic DNA was purified using a DNA blood minikit (Qiagen). PCR products were amplified using a 1:1 mixture of *Taq* DNA polymerase and Expand Long template PCR (Roche).

Transformation of *Toxoplasma gondii* and knockout verification strategy. Electroporations were performed on the model BTX600 electroporator with 1.33×10^7 freshly isolated tachyzoites in the presence of ~15 μg of linearized targeting plasmid DNA as described previously (17). Following selection of parasite clones, the genotypes of clones were validated in PCR assays to measure the following: (i) PCR 1, loss of the deleted coding region of the targeted gene (DF and DR primers); (ii) PCR 2, presence of a target DNA flank (CXF and EXR primers); (iii) PCR 3, correct targeted 5′ integration (CXF and 5′DHFRCXR primers); and (iv) PCR 4, correct targeted 3′ integration (3′DHFRCXF and CXR primers) using a previously described strategy (17).

Single and double knockouts at the OMPDC (Δ*ompdc*) and UP (Δ*up*) loci. The RHΔ*ku80*Δ*hxgprt* strain was transfected with SpeI-linearized pOMT2-2 or with SpeI-linearized pNUPT1-1, and knockouts were continuously selected in MPA (25 μg/ml), xanthine (250 μM), and uracil (250 μM) to isolate the cloned strains RHΔ*ku80*Δ*ompdc*::*hxgprt* and RHΔ*ku80*Δ*up*::*hxgprt*, respectively. To remove the HXGPRT minigene cassette from the RHΔ*ku80*Δ*ompdc*::*hxgprt* strain, parasites were transfected with SpeI-linearized pOMC2-4 and selected in 6TX (250 μg/ml) and uracil (250 μM). Strain RHΔ*ku80*Δ*ompdc*Δ*hxgprt* was validated using PCR 5 with a forward primer (CLOMF) designed in the 3′ side of the 5′ targeting flank and the CXR primer. The strain was transfected with SpeI-linearized pNUPT1-1, and the strain RHΔ*ku80*Δ*ompdc*Δ*up*::*hxgprt* was selected in MPA, xanthine, and uracil medium.

Functional complementation of strain RHΔ*ku80*Δ*ompdc*::*hxgprt*. Strain RHΔ*ku80*Δ*ompdc*::*hxgprt* was transfected with the PmeI-linearized plasmid pGUPROMT, containing the 3,229-bp OMPDC locus. Following transfection, the culture was maintained in the presence of uracil (250 μM) for 24 h, uracil medium was removed, and the selection was then continued in the absence of uracil. Parasites emerging from this selection were subcloned, and individual isolates were evaluated for their genotype to verify targeted deletion of UPRT and the simultaneous insertion of a functional allele of OMPDC. The genotype of the expected gene replacement at the UPRT locus was verified in PCR 1 to assay for deletion of UPRT, in PCR 6 to assay for correct integration of the genomic allele of OMPDC (using the primers UPRTCXF and OMXEXR), and by verifying that individual clonal isolates were also uniformly resistant to 5 μM FUDR to demonstrate a functional loss of UPRT.

Virulence assays, immunizations, and challenge infections. Adult 6- to 8-week-old C57BL/6 mice and gamma interferonγ knockout mice, B6.129S7-Ifng^{tm1Ts}/J (IFN-γ$^{-/-}$), were obtained from Jackson Laboratory (Bar Harbor, ME) and maintained in Tecniplast seal-safe mouse cages on vent racks at the Dartmouth-Hitchcock Medical Center (Lebanon, NH, campus) mouse facility. All mice were cared for and handled according to Animal Care and Use Program of Dartmouth College using National Institutes of Health approved Institutional Animal Care and Use Committee guidelines. Groups of 4 mice (C57BL/6) or 3 mice (IFN-γ$^{-/-}$) were injected intraperitoneally (i.p.) with 0.2 ml PBS containing defined numbers of tachyzoites, and mice were then monitored daily for degree of illness and survival. Virulence assays were performed twice. C57BL/6 mice that survived the virulence assay challenge infections were used in subsequent experiments to determine whether mice were immune to lethal challenge infections. Surviving immunized mice were infected i.p. with 200 tachyzoites (LD200) of strain RH 1 month after immunization along with age-matched naive mouse controls, and mice were then monitored daily to determine the degree of illness and survival.

RESULTS

Genetic dissection of pyrimidine synthesis and salvage in *T. gondii*. To further define the functional role of the *de novo* pyrimidine synthesis pathway, we targeted the last step of the pathway encoded by the OMPDC gene (Fig. 1). Targeting OMPDC eliminates the possibility that the parasite can access and salvage any host cell intermediates in the pyrimidine synthesis pathway prior to OMP (Fig. 1). The host cell nucleotides OMP, UMP, and TMP are inaccessible to the parasite via any direct salvage pathway (4, 14). We also targeted the UP activity to functionally address the potential of the pyrimidine salvage pathway to compensate for defects in the biosynthetic pathway (Fig. 1). Targeting UP in the salvage pathway eliminates direct access to host pyrimidine nucleosides (uridine, cytidine, deoxyuridine, and deoxycytidine) that can be transported into the parasite (5). Consequently, phenotypic evaluation of single knockouts at the OMPDC and UP loci in conjunction with evaluation of a double knockout (OMPDC and UP) was predicted to provide a valid test of the current model for pyrimidine synthesis and salvage in *T. gondii* (Fig. 1) (14).

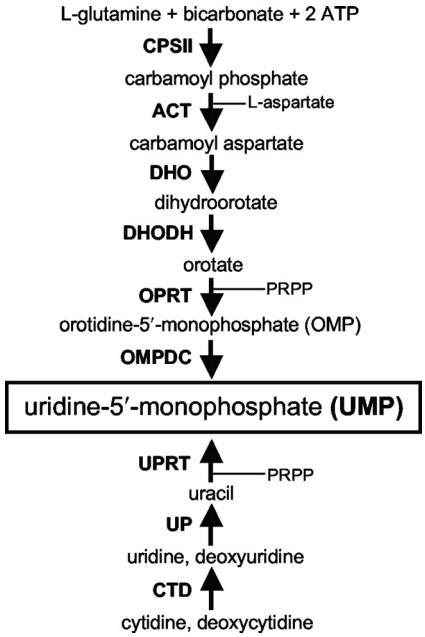

FIG. 1. Model of pyrimidine synthesis and salvage pathways in *Toxoplasma gondii*. Top, arrowheads pointing down: the six-step *de novo* pyrimidine synthesis pathway results in production of UMP. Molecule building and intermediate metabolites are shown (PRPP, phosphoribosyl-1-pyrophosphate). Biosynthetic enzymes mediating each step of the pathway are shown in bold. CPSII, carbamoyl phosphate synthetase II; ACT, aspartate transcarbamoylase; DHO, dihydroorotase; DHODH, dihydroorotate dehydrogenase; OPRT, orotate phosphoribosyltransferase; OMPDC, orotidine-5′-monophosphate decarboxylase. Bottom, arrowheads pointing up: the three-step pyrimidine salvage pathway to UMP. Intermediate metabolites are shown. Salvage enzymes mediating each step of the pathway are shown in bold. UPRT, uracil phosphoribosyltransferase; UP, uridine phosphorylase; CTD, cytidine deaminase.

Targeted deletions were constructed in the OMPDC gene using a strategy (Fig. 2A) based on efficient gene targeting via double-crossover homologous recombination in strain RHΔ*ku80*Δ*hxgprt* (17). The same strategy illustrated in Fig. 2A was also used to create a targeted disruption of the UP gene. The disrupted UP strain (RHΔ*ku80*Δ*ompdc*::*HXGPRT*) exhibited an intracellular growth rate and plaque forming ability identical to that of the parental strain, RHΔ*ku80*::*HXGPRT* (data not shown). Cloned isolates of the ΔOMPDC (strain RHΔ*ku80*Δ*ompdc*::*HXGPRT*) and ΔUP (strain RHΔ*ku80*Δ*up*::*HXGPRT*) knockouts were verified genotypically using a PCR strategy to demonstrate precisely targeted deletion and insertion of the selectable marker HXGPRT at the targeted loci (Fig. 1), (see Materials and Methods; also data not shown). The ΔOMPDC knockout was then retargeted at the disrupted OMPDC locus using the plasmid pOMC2-2, which, while retaining the same 5′ and 3′ target flanks, was deleted for the HXGPRT marker. Transfected ΔOMPDC knockouts were selected in 6TX to select for tar-

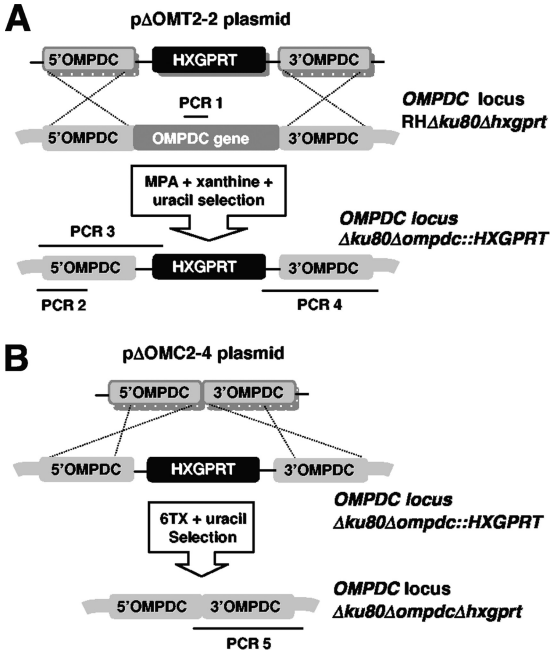

FIG. 2. Targeted gene deletion at the OMPDC locus. (A) Strategy for deletion and validation of the endogenous OMPDC locus via targeted integration of the HXGPRT marker at the OMPDC locus of strain RHΔ*ku80*Δ*hxgprt*. Approximate locations of PCR products used to validate genotypes are depicted. The parental strain, RHΔ*ku80*Δ*hxgprt*, was positive for PCR 1 and PCR 2 products, while the targeted OMPDC knockout was positive only for PCR 2. In addition, the OMPDC knockout strain but not the parental strain was also positive for PCR 3 and PCR 4 products showing correctly targeted integration of HXGPRT and deletion of OMPDC (see Materials and Methods). (B) Strategy for cleanup of the deleted OMPDC locus. The HXGPRT marker was removed from the disrupted OMPDC locus using the depicted strategy that utilized the ability to negatively select against the HXGPRT marker using 6TX after transfection with the pΔOMC2-4 plasmid. Successfully cleaned-up strains with HXGPRT deleted were validated using PCR 5 (see Materials and Methods).

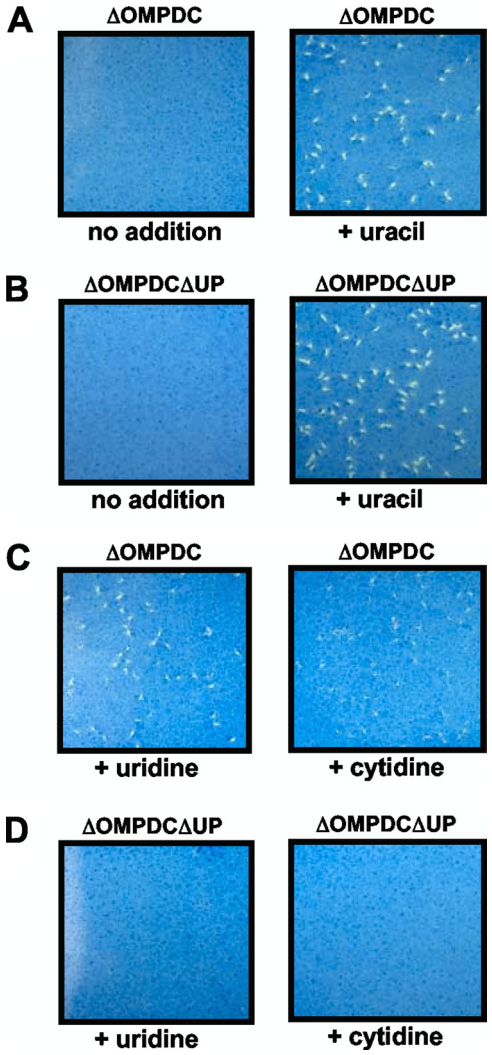

FIG. 3. Functional rescue of pyrimidine auxotrophs in *Toxoplasma gondii*. Approximately 200 tachyzoites of strain RHΔ*ku80* Δ*ompdc*::*HXGPRT* (A and C) or strain RHΔ*ku80*Δ*ompdc* Δ*up*::*HXGPRT* (B and D) were inoculated into a PFU assay in the absence of pyrimidine supplementation (A and B), in the presence of uracil supplementation (200 μM) (A and B), in the presence of uridine supplementation (200 μM) (C and D), or in the presence of cytidine supplementation (200 μM) (C and D) of the growth medium. The culture monolayer was stained 7 days later to reveal PFU and HFF monolayers.

geted removal of the HXGPRT marker from the disrupted OMPDC locus (Fig. 2B). Clones resistant to 6TX were isolated, and the genotype of the ΔOMPDC strain deleted for HXGPRT (strain RHΔ*ku80*Δ*ompdc*Δ*hxgprt*) was confirmed by PCR genotyping (data not shown). The ΔOMPDC strain deleted for HXGPRT was then retargeted using the UP deletion targeting plasmid pNUPT1-1 to generate the double knockout ΔOMPDC ΔUP strain (strain RHΔ*ku80*Δ*ompdc*Δ*up*::*HXGPRT*) (Table 1). The ΔOMPDC and ΔOMPDC ΔUP strains were also evaluated for their reversion frequency using PFU assays performed in the absence of uracil supplementation. As expected, no revertants were detected in multiple independent PFU assays using a total of $\sim 1 \times 10^9$ tachyzoites of the ΔOMPDC or ΔOMPDC ΔUP strain (data not shown).

Functional analysis of pyrimidine synthesis and salvage potential in *T. gondii*. The precisely targeted and deleted ΔOMPDC, ΔUP, and ΔOMPDC ΔUP strains were examined for growth in the absence of uracil supplementation in PFU assays to illustrate the growth phenotypes. The ΔUP strain and the parental KU80 knockout strains replicate normally in the absence and presence of uracil, uridine, or cytidine (data not shown). In contrast, while the growth rates of the ΔOMPDC and ΔOMPDC ΔUP strains were normal in uracil, both strains exhibited a severe pyrimidine auxotrophy and replication deficiency in the absence of uracil supplementation (Fig. 3A and B). In contrast to the complete rescue of growth and PFU observed with uracil supplementation, replication of the ΔOMPDC strain was only partially rescued with high concentrations of uridine and was poorly rescued with high concentrations of cytidine, as revealed by the markedly decreasing sizes of the zones of infection present in the PFU (Fig. 3C). Similar rescue profiles were also observed using deoxyuridine or deoxycytidine, respectively (data not shown). This pyrimidine rescue profile suggested a differential flux of metabolites depending on their point of entry into the salvage pathway

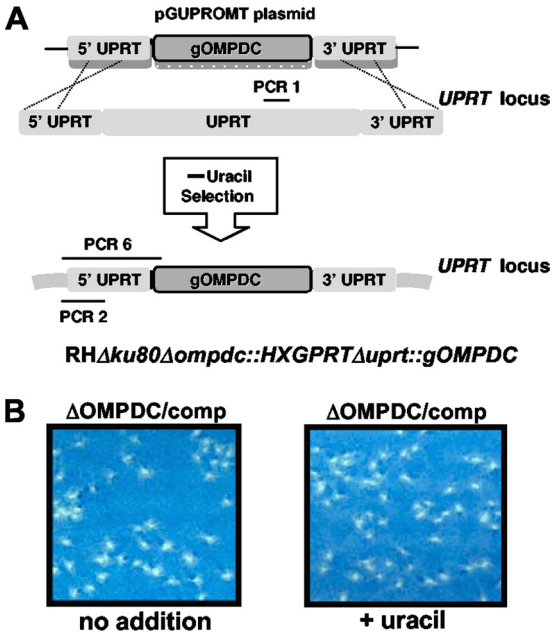

FIG. 4. Complementation of the ΔOMPDC strain. (A) Strategy for complementation of the ΔOMPDC strain by simultaneous knockout of UPRT and targeted insertion of the genomic allele of OMPDC at the UPRT locus. Strain RHΔ*ku80*Δ*ompdc*::*HXGPRT* was transfected with the plasmid pGUPROMT, and parasites that were complemented for *de novo* pyrimidine biosynthesis were selected by growth in medium without uracil supplementation. Approximate locations of PCR 1 (targeted deletion of UPRT) and PCR 6 (targeted integration of the genomic allele of OMPDC) validation products are shown (see Materials and Methods). Correctly targeted replacement clones were positive only for the PCR 2 and PCR 6 products and were negative for PCR 1. The parental strain was positive only for PCR 1 and PCR 2. (B) Functional rescue of complemented strain RHΔ*ku80*Δ*ompdc*::*HXGPRT*Δ*uprt*::gOMPDC. Approximately 200 tachyzoites of strain RHΔ*ku80*Δ*ompdc*::*HXGPRT*Δ*uprt*::*gOMPDC* were assayed in an 8-day PFU assay in the absence (no addition) or presence of uracil.

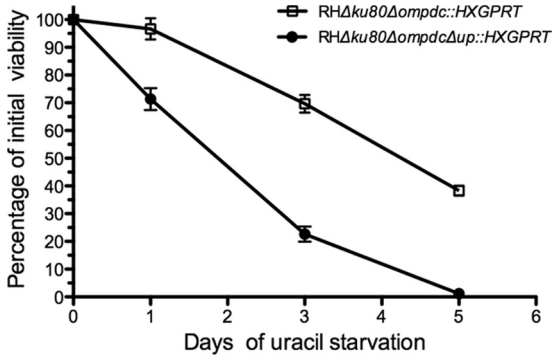

FIG. 5. Pyrimidine starvation causes a rapid loss of parasite viability. PFU assays were used to measure how rapidly pyrimidine auxotrophs lost viability intracellularly under conditions of pyrimidine starvation in a 5-day starvation assay. Viability profiles for the ΔOMPDCΔUP knockout strain (solid circles) and the ΔOMPDC knockout strain (open squares) are shown.

(Fig. 1). Collectively, these results demonstrated that in the ΔOMPDC background, the parasite-encoded UP provided at least partial functional rescue of parasite growth of pyrimidine auxotrophs *in vitro* through conversion of uridine to uracil or minor rescue through cytidine that was first converted to uridine by a cytidine deaminase (CTD) activity if extremely high concentrations of uridine or cytidine, respectively, were exogenously supplied in culture medium (Fig. 1).

To definitively demonstrate that the parasite UP acted in the salvage pathway depicted in Fig. 1 rather than via any potential alternative pathway to partially rescue pyrimidine auxotrophy *in vitro*, we examined the double knockout ΔOMPDC ΔUP strain in the same PFU rescue assays (Fig. 3D). Growth rescue was not observed in the ΔOMPDC ΔUP strain using either 200 μM uridine or 200 μM cytidine supplementation or by supplementing medium with 4 mM concentrations of uridine or cytidine (data not shown). Replication of the ΔOMPDC ΔUP strain could be rescued only by uracil supplementation *in vitro* (Fig. 3B).

Complementation of pyrimidine auxotrophy. Genotyping of the ΔOMPDC, ΔUP, and ΔOMPDC ΔUP knockout strains indicated precise disruption of the targeted loci in the KU80 knockout background. To demonstrate that the knockout strains had precisely targeted deletions with no unknown pleiotropic or epigenetic alterations that could potentially influence the phenotype(s) under observation, we functionally complemented the pyrimidine auxotrophy. A functional wild-type allele of the OMPDC gene was inserted by targeted gene replacement into the UPRT locus, simultaneously deleting the coding region of the UPRT gene (Fig. 4A). Since the rescue of pyrimidine auxotrophy in *T. gondii* is completely dependent on UPRT (Fig. 1) (14), selection of targeted ΔOMPDC strains is feasible in the absence of uracil only if functional complementation is successful. The complemented ΔOMPDC strain RHΔ*ku80*Δ*ompdc*::*HXGPRT*Δ*uprt*::*gOMPDC* (Table 1) was disrupted in UPRT and was resistant to FUDR, and the growth rate of the complemented strain was normal whether uracil was absent or present in culture medium (Fig. 4B).

Pyrimidine starvation causes a rapid loss of viability. PFU assays were used to measure how rapidly pyrimidine auxotrophs lost viability intracellularly under conditions of pyrimidine starvation. When subjected to pyrimidine starvation, the ΔOMPDC ΔUP knockout strain lost viability at a markedly higher rate than the ΔOMPDC knockout strain (Fig. 5). A significant loss in viability of the ΔOMPDC ΔUP knockout was detected as early as 1 day after initiation of pyrimidine starvation. After 5 days of pyrimidine starvation, the viability of the ΔOMPDC ΔUP knockout strain was reduced to 1.1% ± 0.6% of the initial viability, whereas that of the ΔOMPDC knockout strain was reduced to 38% ± 1.8% of the initial viability (Fig. 5).

Pyrimidine biosynthesis is required for virulence. The attenuation of virulence of the nonreverting ΔOMPDC, ΔUP, and ΔOMPDC ΔUP knockout strains was evaluated. C57BL/6 mice inoculated intraperitoneally (i.p.) with a dose of 20 tachyzoites of the parental strain RHΔ*ku80*::*HXGPRT* or with a dose of 20 tachyzoites of the ΔUP strain uniformly succumbed to virulent infection (Fig. 6A). In contrast, C57BL/6 mice inoculated i.p. with a dose of 1×10^6, 1×10^7, or 5×10^7 tachyzoites of either the ΔOMPDC strain or the ΔOMPDC ΔUP strain uniformly survived each of these extremely high-dose parasite challenges (Fig. 6A). Homozygous IFN-$\gamma^{-/-}$ mice uniformly survived a challenge dose of 1×10^7 ΔOMPDC

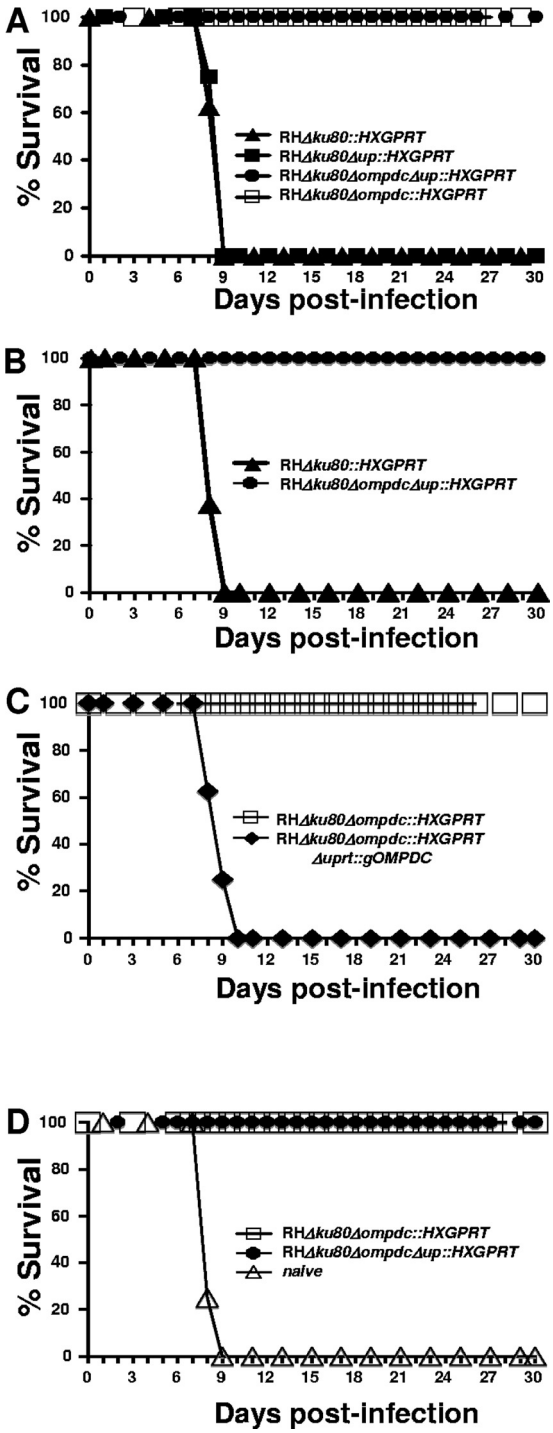

FIG. 6. Pyrimidine auxotrophs are severely attenuated in virulence and elicit potent immunity to *T. gondii*. (A) Groups of C57BL/6 mice were inoculated i.p. with 20 tachyzoites of strain RHΔ*ku80*::*HXGPRT* (solid triangles), 20 tachyzoites of strain RHΔ*up*::*HXGPRT* (solid squares), 1×10^6, 1×10^7, or 5×10^7 tachyzoites of strain RHΔ*ku80*Δ*ompdc*::*HXGPRT* (open squares) (each dose is shown by the same symbol), or 1×10^6, 1×10^7, or 5×10^7 tachyzoites of strain RHΔ*ku80*Δ*ompdc*Δ*up*::*HXGPRT* (solid circles) (each dose is shown by the same symbol). (B) Groups of IFN-$\gamma^{-/-}$ mice were inoculated i.p. with 20 tachyzoites of RHΔ*ku80*::*HXGPRT* (solid triangles) or with 1×10^7 tachyzoites of strain RHΔ*ku80*Δ*ompdc*Δ*up*::*HXGPRT* (solid circles). (C) Groups of C57BL/6 mice were inoculated i.p. with 20 tachyzoites of strain RHΔ*ku80*Δ*ompdc*::*HXGPRT*Δ*uprt*::*gOMPDC* (solid diamonds) or with 1×10^7 tachyzoites of RHΔ*ku80*Δ*ompdc*::*HXGPRT* (open squares). (D) Thirty days after i.p. injection of parasites, all groups of C57/BL6 mice uniformly surviving the RHΔ*ku80*Δ*ompdc*::*HXGPRT* (open squares) and RHΔ*ku80*Δ*ompdc*Δ*up*::*HXGPRT* (solid circles) inoculations (1×10^6-, 1×10^7-, or 5×10^7-tachyzoite doses from panel A) were challenged with a lethal dose of 200 tachyzoites of hypervirulent strain RH. Naive age-matched mice (open triangles) were given the same lethal challenge. Mice were monitored over a 30-day period for health and survival.

ΔUP tachyzoites (Fig. 6B). Significantly, extreme virulence was restored in the complemented uracil auxotroph strain RHΔ*ku80*Δ*ompdc*::*HXGPRT*Δ*uprt*::*gOMPDC* (Fig. 6C).

ΔOMPDC and ΔOMPDC ΔUP strains elicit protective immunity against virulent *T. gondii* infection. To examine the potential of the ΔOMPDC and ΔOMPDC ΔUP strains to serve as vaccines, C57BL/6 mice that survived the initial challenge infections with these strains were rechallenged 30 days later with 200 tachyzoites of strain RH (LD200). All mice vaccinated with a single dose of 1×10^6, 1×10^7, or 5×10^7 tachyzoites of the ΔOMPDC strain or the ΔOMPDC ΔUP strain uniformly survived lethal RH challenge infection (Fig. 6D). In contrast, all naive C57BL/6 mice rapidly succumbed to the lethal RH challenge infection.

DISCUSSION

Insertional disruption of the first step of the *de novo* pyrimidine synthesis pathway, encoded by the CPSII gene, produced severe uracil auxotrophic mutants of *T. gondii* that were incapable of *de novo* pyrimidine synthesis (13–16). After invasion of a host cell, the cps1-1 uracil auxotrophic mutant was starved for pyrimidines and did not replicate. However, the cps1-1 strain is not easily amenable to further genetic manipulation, and the disruption in CPSII in this strain is insertional rather than deletional (13). To develop improved nonreverting, avirulent, and well-defined strains that are more easily amenable to additional defined genetic manipulations, we utilized recently developed KU80 knockout strains (17) to precisely target and delete the gene encoding the final step of the pyrimidine biosynthetic pathway, the OMPDC activity. We also examined the functional capacity of the pyrimidine salvage pathways by deleting the UP salvage activity, which controls the direct access to host cell pyrimidine nucleosides (26), with or without an intact pyrimidine biosynthetic pathway. The parasite UP activity is nonspecific and is active on uridine, deoxyuridine, and thymidine (26).

As predicted from the current model for *T. gondii* pyrimidine pathways (Fig. 1), disruption of the UP activity had no effect on parasite growth or virulence. In contrast, disruption of OMPDC in the ΔOMPDC strain produced a severe uracil auxotrophy due to the loss of UMP derived from the *de novo* pyrimidine synthesis pathway. Rescue of the UMP pool from the salvage pathway minimally requires parasite UPRT and pyrimidine supplementation to the growth medium. The nucleobase uracil provided the most effective functional rescue of the UMP pool, and uracil supplementation restored a normal growth rate in the ΔOMPDC strain. The replication of the ΔOMPDC strain was also partially rescued with high concen-

trations of uridine and was detectably but poorly rescued with high concentrations of cytidine. This pyrimidine rescue profile suggested a differential flux of metabolites depending on their point of entry into the salvage pathway. Since cytidine must be first converted to uridine by a CTD activity, this nucleoside provides reduced rescue compared to that of uridine, and also, uridine provided reduced rescue compared to that of uracil. Similar rescue results were observed for deoxyuridine and deoxycytidine, respectively, consistent with previous evidence showing the parasite UP and CTD activities are active on both the ribonucleoside and the deoxyribonucleoside (11, 25).

T. gondii has no detectable pyrimidine nucleoside kinase activity (26), and cleavage of nucleosides is due to nucleoside phosphorylase activities rather than any prominent nucleoside hydrolase activity (25). Additionally, no detectable pathway to transport or directly salvage host cell pyrimidine nucleotides exists (5, 14). Consequently, we conclude that the potential salvage of host cell uracil and nucleosides (cytidine, deoxycytidine, uridine, and deoxyuridine) is not sufficient to support a significant rate of parasite replication in mammalian cells *in vitro* in pyrimidine auxotroph backgrounds created by disruption of the OMPDC activity in the biosynthetic pathway.

Our study did not define whether the CTD that converts cytidine to uridine is a host cell-encoded enzyme or a parasite-encoded enzyme. The genome of *T. gondii* predicts a putative gene locus for a potential CTD gene (TGGT1_051230), and as mentioned, a CTD activity has been previously found in isolated tachyzoites (25). However, because the enzyme activity originally reported for the CTD was very low (25), the possibility of host cell contamination of the enzyme preparations cannot be completely discounted and a genetic approach is still necessary to conclusively address the functional origin of the CTD that partially rescues growth of the ΔOMPDC pyrimidine auxotroph in this study. Rescue of pyrimidine auxotrophy using exogenously supplied uracil or pyrimidine nucleosides minimally also mechanistically requires parasite plasma membrane transporters for these pyrimidines, and nucleobase and nucleoside transporters have been found in *T. gondii* (5). Our study also did not address whether host cell transporters are necessary for salvage of exogenously supplied pyrimidines.

While growth of the ΔOMPDC ΔUP strain was also rescued completely by uracil supplementation, replication of this double knockout was not rescued by supplementation of growth medium with either uridine or cytidine or their corresponding deoxyribonucleosides. These results definitively demonstrate that the salvage of all host cell-derived pyrimidine nucleosides (cytidine, deoxycytidine, uridine, and deoxyuridine) into the UMP pool of the parasite is dependent on the sequential action of the parasite-encoded UP and UPRT activities. These results suggest that the infected host cell UP activity does not play any significant role in supporting parasite replication by providing uracil to the pyrimidine salvage pathway of the intracellular parasite. However, our experiments do not exclude the possibility that the parasite has limited access to host cell uracil made available through the activity of the host cell-encoded UP, but if so, the biochemical flux of this pathway is not sufficient to support parasite replication.

Previous biochemical and genetic results implicated a potentially significant role of the parasite-specific pathway in salvage of pyrimidines (4, 13, 14, 25, 35), although it has still been poorly understood how the biosynthetic and salvage pathways are integrated and regulated. The ability to now more rapidly and reliably target gene knockouts and gene replacements in the KU80 knockout background should accelerate progress in understanding the pyrimidine pathways, as well as essential purine salvage and other nutritional pathways critical to intracellular parasite survival and growth (17). Simultaneous complementation of pyrimidine auxotrophy and targeted disruption of UPRT (ΔUPRT) with a functional allele of OMPDC in the ΔOMPDC background now conclusively demonstrate that *T. gondii* can grow normally with UMP derived from a fully functional *de novo* pyrimidine synthesis pathway while having no functional pyrimidine salvage pathway. Conversely, if a ΔOMPDC or ΔOMPDCΔUP pyrimidine auxotroph strain is provided with high levels of the pyrimidine supplement uracil in growth medium *in vitro*, the parasite can also grow normally while deriving UMP from the pyrimidine salvage pathway in the absence of any functional biosynthetic pathway.

The absence of UP has no apparent effect on parasite growth or virulence. However, our assays of viability following pyrimidine starvation demonstrate that the presence or absence of UP in pyrimidine auxotrophs is correlated with viability. After 5 days of pyrimidine starvation, the ΔOMPDC knockout strain retained 38% ± 1.8% viability while the ΔOMPDC ΔUP double knockout strain retained only 1.1% ± 0.6% viability. Our previous kinetic analysis of pyrimidine starvation showed that after 5 days of pyrimidine starvation, the cps1-1 strain retained ~25% viability (13). Collectively, these observations suggest that the loss of viability of ΔOMPDC knockouts during pyrimidine starvation is significantly accelerated in the absence of the parasite UP activity.

The essential nature of *de novo* pyrimidine synthesis, the extremely limited functional capacities of the pyrimidine salvage pathway in infected host cells in the absence of pyrimidine supplementation *in vitro*, and evidence suggesting that uracil is not readily available in mammals (12, 13, 32) collectively explain the remarkable attenuation of growth *in vitro* and attenuation of virulence in mice that we observed in the ΔOMPDC and ΔOMPDC ΔUP strains. The attenuation in virulence of these nonreverting pyrimidine auxotroph strains approaches ~8 logs (or more) compared to the virulent parent RH strain, where a single viable parasite is lethal to mice (36). The ΔOMPDC ΔUP strain also exhibits extreme attenuation in IFN-$\gamma^{-/-}$ mice, suggesting that the growth disruption in this background is severe *in vivo*. Uracil auxotrophy is a profoundly effective strategy to eliminate virulence in *T. gondii* infection.

A single immunization of mice with the ΔOMPDC strain or the ΔOMPDC ΔUP strain elicited a completely protective immunity to lethal challenge infection. The cps1-1 strain elicits a potent $CD8^+$ T-cell-dependent protective immunity (13, 18, 19, 28, 39, 41) that confers lifelong immunity against infection with type I strains (13, 18), as well as lifelong immunity against infection with type II strains and chronic infection (19). The cps1-1-induced immunity is dependent on IL-12 (18, 41, 44) and is also dependent on IFN-γ (13, 18), although systemic IFN-γ is not required for priming this immunity (18). This priming of immunity is characterized by four distinct effector $CD8^+$ T-cell types based on KLRG1 and CD62L expression levels (44) that produce abundant populations of antigen-spe-

cific $CD8^+$ T cells that are cytolytic *in vitro* and *in vivo* (28) and also elicits effective generation of memory $CD8^+$ T cells (43, 44). Recently the $CD8^+$ T-cell-dependent immunity elicited by the attenuated cps1-1 uracil auxotroph strain, which actively invades the host cell but does not subsequently replicate, was reported to arise unexpectedly with much faster kinetics than that observed with replicating strains that actively lyse the infected cell (28). Surprisingly, the early cytokine response to the type I uracil auxotroph strain cps1-1 also resembles the characteristic response of a type II strain in regard to early production of IL-12 (18). RH challenge parasites are not detected in cps1-1-vaccinated mice by ~3 weeks after challenge, and the genomes of tachyzoites from the original cps1-1 vaccination also are not detected at the same time the RH challenge parasites are assayed (18, 28). While the ΔOMPDC and ΔOMPDC ΔUP strains elicit an effective protective immune response against lethal RH challenge, additional experiments are needed to determine whether long-term immunity is elicited and whether these new strains can be further manipulated to elicit a protective antigen-based response against other pathogens in naive mice or in mice already immune to *T. gondii*.

Our study provides further evidence that the *de novo* pyrimidine synthesis pathway of *T. gondii* is essential and that this pathway provides an excellent target for vaccine design and chemotherapy. This study defines and validates potentially improved, extremely attenuated, nonreverting, genetically defined, and now genetically manipulatable strains developed in the KU80 knockout background that enable precise and efficient gene targeting via homologous recombination (17). The ΔOMPDC and ΔOMPDC ΔUP strains developed in this study should also provide new tools for the further biological dissection of innate and adaptive host responses to *T. gondii* infection. Significantly, the newly developed nonreverting avirulent uracil auxotroph strains reported here now potentially provide an excellent vaccine platform strategy in which to examine engineered antigens or $CD8^+$ T-cell epitopes of interest that can elicit potent Th1 and other relevant immune responses to combat significant global infectious diseases that have been remarkably resistant to previous vaccination strategies.

ACKNOWLEDGMENTS

This work was supported by NIH grants (AI073142, AI075931, and AI41930).

The work of the developers of the *Toxoplasma gondii* Genome Resource at www.ToxoDB.org is gratefully acknowledged. ToxoDB, PlasmoDB, and EuPathDB are part of the NIH/NIAID-funded Bioinformatics Resource Center. We thank Leah M. Rommereim, Alejandra Falla, and Kiah Sanders for helpful discussions.

REFERENCES

1. **Asai, T., W. J. O'Sullivan, M. Kobayashi, A. M. Gero, M. Yokogawa, and M. Tatibana.** 1983. Enzymes of the de novo pyrimidine biosynthetic pathway in *Toxoplasma gondii*. Mol. Biochem. Parasitol. **7:**89–100.
2. **Butcher, B. A., and E. Y. Denkers.** 2002. Mechanism of entry determines the ability of *Toxoplasma gondii* to inhibit macrophage proinflammatory cytokine production. Infect. Immun. **70:**5216–5224.
3. **Charles, E., S. Joshi, J. D. Ash, B. A. Fox, A. D. Farris, D. J. Bzik, M. L. Lang, and I. J. Blader.** 24 May 2010. CD4 T-cell suppression by cells from *Toxoplasma gondii*-infected retinas is mediated by PD-L1. Infect. Immun. doi:10.1128/IAI.00117-10.
4. **Chaudhary, K., B. A. Fox, and D. J. Bzik.** 2007. *Toxoplasma gondii*: the model apicomplexan parasite: perspectives and methods. Elsevier, London, United Kingdom.
5. **De Koning, H. P., M. I. Al-Salabi, A. M. Cohen, G. H. Coombs, and J. M. Wastling.** 2003. Identification and characterisation of high affinity nucleoside and nucleobase transporters in *Toxoplasma gondii*. Int. J. Parasitol. **33:**821–831.
6. **Donald, R. G., D. Carter, B. Ullman, and D. S. Roos.** 1996. Insertional tagging, cloning, and expression of the *Toxoplasma gondii* hypoxanthine-xanthine-guanine phosphoribosyltransferase gene. Use as a selectable marker for stable transformation. J. Biol. Chem. **271:**14010–14019.
7. **Donald, R. G., and D. S. Roos.** 1998. Gene knock-outs and allelic replacements in *Toxoplasma gondii*: HXGPRT as a selectable marker for hit-and-run mutagenesis. Mol. Biochem. Parasitol. **91:**295–305.
8. **Donald, R. G., and D. S. Roos.** 1995. Insertional mutagenesis and marker rescue in a protozoan parasite: cloning of the uracil phosphoribosyltransferase locus from *Toxoplasma gondii*. Proc. Natl. Acad. Sci. U. S. A. **92:**5749–5753.
9. **Dubey, J. P., D. S. Lindsay, and C. A. Speer.** 1998. Structures of *Toxoplasma gondii* tachyzoites, bradyzoites, and sporozoites and biology and development of tissue cysts. Clin. Microbiol. Rev. **11:**267–299.
10. **Dzierszinski, F., M. Pepper, J. S. Stumhofer, D. F. LaRosa, E. H. Wilson, L. A. Turka, S. K. Halonen, C. A. Hunter, and D. S. Roos.** 2007. Presentation of *Toxoplasma gondii* antigens via the endogenous major histocompatibility complex class I pathway in nonprofessional and professional antigen-presenting cells. Infect. Immun. **75:**5200–5209.
11. **el Kouni, M. H., F. N. Naguib, R. P. Panzica, B. A. Otter, S. H. Chu, G. Gosselin, C. K. Chu, R. F. Schinazi, Y. F. Shealy, N. Goudgaon, A. A. Ozerov, T. Ueda, and M. H. Iltzsch.** 1996. Effects of modifications in the pentose moiety and conformational changes on the binding of nucleoside ligands to uridine phosphorylase from *Toxoplasma gondii*. Biochem. Pharmacol. **51:**1687–1700.
12. **Fields, P. I., R. V. Swanson, C. G. Haidaris, and F. Heffron.** 1986. Mutants of Salmonella typhimurium that cannot survive within the macrophage are avirulent. Proc. Natl. Acad. Sci. U. S. A. **83:**5189–5193.
13. **Fox, B. A., and D. J. Bzik.** 2002. De novo pyrimidine biosynthesis is required for virulence of *Toxoplasma gondii*. Nature **415:**926–929.
14. **Fox, B. A., K. Chaudhary, and D. J. Bzik.** 2007. Toxoplasma: molecular and cellular biology. Horizon Bioscience, Norwich, United Kingdom.
15. **Fox, B. A., J. P. Gigley, and D. J. Bzik.** 2004. *Toxoplasma gondii* lacks the enzymes required for de novo arginine biosynthesis and arginine starvation triggers cyst formation. Int. J. Parasitol. **34:**323–331.
16. **Fox, B. A., J. G. Ristuccia, and D. J. Bzik.** 2009. Genetic identification of essential indels and domains in carbamoyl phosphate synthetase II of *Toxoplasma gondii*. Int. J. Parasitol. **39:**533–539.
17. **Fox, B. A., J. G. Ristuccia, J. P. Gigley, and D. J. Bzik.** 2009. Efficient gene replacements in *Toxoplasma gondii* strains deficient for nonhomologous end joining. Eukaryot. Cell **8:**520–529.
18. **Gigley, J. P., B. A. Fox, and D. J. Bzik.** 2009. Cell-mediated immunity to *Toxoplasma gondii* develops primarily by local Th1 host immune responses in the absence of parasite replication. J. Immunol. **182:**1069–1078.
19. **Gigley, J. P., B. A. Fox, and D. J. Bzik.** 2009. Long-term immunity to lethal acute or chronic type II *Toxoplasma gondii* infection is effectively induced in genetically susceptible C57BL/6 mice by immunization with an attenuated type I vaccine strain. Infect. Immun. **77:**5380–5388.
20. **Goldszmid, R. S., I. Coppens, A. Lev, P. Caspar, I. Mellman, and A. Sher.** 2009. Host ER-parasitophorous vacuole interaction provides a route of entry for antigen cross-presentation in *Toxoplasma gondii*-infected dendritic cells. J. Exp. Med. **206:**399–410.
21. **Gubbels, M. J., B. Striepen, N. Shastri, M. Turkoz, and E. A. Robey.** 2005. Class I major histocompatibility complex presentation of antigens that escape from the parasitophorous vacuole of *Toxoplasma gondii*. Infect. Immun. **73:**703–711.
22. **Hill, D. E., S. Chirukandoth, and J. P. Dubey.** 2005. Biology and epidemiology of *Toxoplasma gondii* in man and animals. Anim. Health Res. Rev. **6:**41–61.
23. **Holland, G. N.** 2003. Ocular toxoplasmosis: a global reassessment. Part I: epidemiology and course of disease. Am. J. Ophthalmol. **136:**973–988.
24. **Huynh, M. H., and V. B. Carruthers.** 2009. Tagging of endogenous genes in a *Toxoplasma gondii* strain lacking Ku80. Eukaryot. Cell **8:**530–539.
25. **Iltzsch, M. H.** 1993. Pyrimidine salvage pathways in Toxoplasma gondii. J. Eukaryot. Microbiol. **40:**24–28.
26. **Iltzsch, M. H., and E. E. Klenk.** 1993. Structure-activity relationship of nucleobase ligands of uridine phosphorylase from *Toxoplasma gondii*. Biochem. Pharmacol. **46:**1849–1858.
27. **Jones, J. L., and G. N. Holland.** 2010. Annual burden of ocular toxoplasmosis in the United States. Am. J. Trop. Med. Hyg. **82:**464–465.
28. **Jordan, K. A., E. H. Wilson, E. D. Tait, B. A. Fox, D. S. Roos, D. J. Bzik, F. Dzierszinski, and C. A. Hunter.** 2009. Kinetics and phenotype of vaccine-induced CD8+ T-cell responses to *Toxoplasma gondii*. Infect. Immun. **77:**3894–3901.
29. **Kim, K., and L. M. Weiss.** 2004. *Toxoplasma gondii*: the model apicomplexan. Int. J. Parasitol. **34:**423–432.
30. **Ling, Y. M., M. H. Shaw, C. Ayala, I. Coppens, G. A. Taylor, D. J. Ferguson, and G. S. Yap.** 2006. Vacuolar and plasma membrane stripping and auto-

phagic elimination of *Toxoplasma gondii* in primed effector macrophages. J. Exp. Med. **203:**2063–2071.
31. **Luft, B. J., and J. S. Remington.** 1992. Toxoplasmic encephalitis in AIDS. Clin. Infect. Dis. **15:**211–222.
32. **Mahan, M. J., J. M. Slauch, and J. J. Mekalanos.** 1993. Selection of bacterial virulence genes that are specifically induced in host tissues. Science **259:**686–688.
33. **Oldenburg, K. R., K. T. Vo, S. Michaelis, and C. Paddon.** 1997. Recombination-mediated PCR-directed plasmid construction in vivo in yeast. Nucleic Acids Res. **25:**451–452.
34. **O'Sullivan, W. J., A. M. Johnson, K. G. Finney, A. M. Gero, E. Hagon, J. W. Holland, and G. W. Smithers.** 1981. Pyrimidine and purine enzymes in *Toxoplasma gondii*. Aust. J. Exp. Biol. Med. Sci. **59:**763–767.
35. **Pfefferkorn, E. R.** 1978. *Toxoplasma gondii*: the enzymic defect of a mutant resistant to 5-fluorodeoxyuridine. Exp. Parasitol. **44:**26–35.
36. **Pfefferkorn, E. R., and L. C. Pfefferkorn.** 1976. *Toxoplasma gondii*: isolation and preliminary characterization of temperature-sensitive mutants. Exp. Parasitol. **39:**365–376.
37. **Sabin, A. B.** 1941. Toxoplasmic encephalitis in children. JAMA **116:**801–807.
38. **Schwartzman, J. D., and E. R. Pfefferkorn.** 1981. Pyrimidine synthesis by intracellular *Toxoplasma gondii*. J. Parasitol. **67:**150–158.
39. **Shaw, M. H., G. J. Freeman, M. F. Scott, B. A. Fox, D. J. Bzik, Y. Belkaid, and G. S. Yap.** 2006. Tyk2 negatively regulates adaptive Th1 immunity by mediating IL-10 signaling and promoting IFN-gamma-dependent IL-10 reactivation. J. Immunol. **176:**7263–7271.
40. **Subauste, C. S., and M. Wessendarp.** 2000. Human dendritic cells discriminate between viable and killed *Toxoplasma gondii* tachyzoites: dendritic cell activation after infection with viable parasites results in CD28 and CD40 ligand signaling that controls IL-12-dependent and -independent T cell production of IFN-gamma. J. Immunol. **165:**1498–1505.
41. **Sukhumavasi, W., C. E. Egan, A. L. Warren, G. A. Taylor, B. A. Fox, D. J. Bzik, and E. Y. Denkers.** 2008. TLR adaptor MyD88 is essential for pathogen control during oral *Toxoplasma gondii* infection but not adaptive immunity induced by a vaccine strain of the parasite. J. Immunol. **181:**3464–3473.
42. **Weiss, L. M., and K. Kim.** 2000. The development and biology of bradyzoites of *Toxoplasma gondii*. Front. Biosci. **5:**D391–D405.
43. **Wilson, D. C., G. M. Grotenbreg, K. Liu, Y. Zhao, E. M. Frickel, M. J. Gubbels, H. L. Ploegh, and G. S. Yap.** 2010. Differential regulation of effector- and central-memory responses to *Toxoplasma gondii* infection by IL-12 revealed by tracking of Tgd057-specific CD8+ T cells. PLoS Pathog. **6:**e1000815.
44. **Wilson, D. C., S. Matthews, and G. S. Yap.** 2008. IL-12 signaling drives CD8+ T cell IFN-gamma production and differentiation of KLRG1+ effector subpopulations during *Toxoplasma gondii* infection. J. Immunol. **180:**5935–5945.
45. **Yap, G. S., Y. Ling, and Y. Zhao.** 2007. Autophagic elimination of intracellular parasites: convergent induction by IFN-gamma and CD40 ligation? Autophagy **3:**163–165.
46. **Zhao, Y., D. J. Ferguson, D. C. Wilson, J. C. Howard, L. D. Sibley, and G. S. Yap.** 2009. Virulent *Toxoplasma gondii* evade immunity-related GTPase-mediated parasite vacuole disruption within primed macrophages. J. Immunol. **182:**3775–3781.
47. **Zhao, Y., D. Wilson, S. Matthews, and G. S. Yap.** 2007. Rapid elimination of *Toxoplasma gondii* by gamma interferon-primed mouse macrophages is independent of CD40 signaling. Infect. Immun. **75:**4799–4803.

Editor: J. H. Adams